Intensity fluctuation spectroscopy with coherent X-rays

Eric Dufresne
Centre for the Physics of Materials
Department of Physics, McGill University
Montréal, Québec, Canada

A Thesis submitted to the
Faculty of Graduate Studies and Research
in partial fulfillment of the requirements for the degree of
Doctor of Philosophy

Je dédie cette thèse à mon amour, à ma famille, et à mon grand-père.

Contents

List of common symbols **ix**

Résumé **x**

Abstract **xi**

Acknowledgments **xii**

1 Introduction **1**

2 Coherent X-rays **7**

2.1 Definitions of coherence 7
2.2 Properties of synchrotron radiation 9
2.3 X-ray scattering 11
2.4 X-ray scattering from Cu_3Au 15
2.5 Production of coherent X-rays: experimental method 19
2.5.1 Coherence volume 23
2.6 Structure factor with coherent X-rays 24
2.6.1 Coherent X-ray scattering for the study of isolated defects or artificially made structures 25
2.6.2 Scattering from a binary alloy in equilibrium 28

3 Characterization of position-sensitive detectors **40**

3.0.3 Description of the technique 41
3.0.4 Characterization of a linear PSD 48
3.0.5 Characterization of a CCD array 53
3.0.6 Discussion 61

4 Experimental method **63**

4.1 Beamline characterization and optics 63
4.2 Sample preparation and sample furnace 65
4.3 Scattering geometry 66
4.4 Data treatment 67
4.5 Pinhole construction 68
4.6 Demonstration of coherence: Fraunhofer diffraction pattern of a pinhole. 69
4.7 Incident X-ray beam structure and stability 72
4.8 Temperature calibration and heat treatment 75
4.9 Setting the angle of incidence θ_i 76

5 RESULTS **78**
5.1 Static speckle patterns 78
5.1.1 Measuring speckle size 83
5.1.2 Contrast 92
5.2 Ordering kinetics of an order-disorder phase transition 94
5.2.1 Numerical Simulations of model A 110

6 CONCLUSIONS **118**

APPENDICES **124**
A.1 Some useful probability distributions 124
A.2 Error analysis 125
A.2.1 Uncertainty in the measured mean and variance 126
A.2.2 Correlation of the sample mean and variance 127
A.2.3 Evaluation of the error on a function of S^2 and $<x>$ 128
A.2.4 Including electronic noise for an X-ray detector 128
A.3 Derivation of the autocorrelation function for a Gaussian 130
A.4 Tools for time fluctuations analysis 130

REFERENCES **133**

Figures and Tables

Figures

2.1 Fraunhofer and Bragg condition 12
2.2 An order-disorder transition 16
2.3 Superlattice anisotropy 18
2.4 The experimental setup. 20
2.5 Energy dependence of scattering in Cu_3Au 23
2.6 Longitudinal coherence condition. 24
2.7 Structure factor of an edge dislocation 26
2.8 Structure factor with coherent illumination. 31
2.9 A slice of Fig 2.8. 32
2.10 The scattering amplitude for speckle 33
2.11 IFS on model A. 35
2.12 Probability density of $S(\vec{q})$. 36
2.13 The statistic of the time-averaged intensity. 38

3.1 Ratio of variance over mean 50
3.2 Spatial correlation function $C(i, \Delta)$ 51
3.3 Detector calibration setup 54
3.4 Ratio of variance over mean for CCD 55
3.5 Detector calibration curve 55
3.6 Variance of the linearized signal 56
3.7 Spatial uniformity of the row or column average 57
3.8 Time averaged variance 58
3.9 Slices of the time averaged variance 59
3.10 The spatial correlation function for the CCD 60

4.1 The X-ray oven 65
4.2 The scattering geometry 67
4.3 The CCD calibration at CHESS and X25 68
4.4 Fraunhofer diffraction patterns of a 7.5 μm pinhole along $2\Theta_{||}$ and $2\Theta_{\perp}$ 70
4.5 Fraunhofer diffraction measured with a CCD 73
4.6 Time fluctuations of the incident beam at X25 74
4.7 Horizontal and vertical structure of the incident beam at X25 75
4.8 Square of the order parameter versus temperature, and the quench profile for a typical quench 76

5.1 A typical static speckle pattern from Cu3Au (100) 79
5.2 Speckle patterns dependence on X-ray optics. 82

5.3 Autocorrelation function for Cu_3Au (100) 84
5.4 Slices of $\Gamma(\vec{\Delta q}, t, 0)$ 85
5.5 The detector crosscorrelation 86
5.6 Comparison of Eq. 5.7 and Eq. 5.8 87
5.7 The speckle size for different optical conditions 89
5.8 Variations of the correlation function maximum with pinhole diameter 90
5.9 The contrast for different optical conditions 93
5.10 $S(\vec{q}, t)$ for three different times in run 21 95
5.11 Slices of $S(\vec{q}, t)$ along $2\theta_\perp$ and $2\theta_\|$ in Fig. 5.10 97
5.12 Fit parameters for the data collected at X25 and CHESS 98
5.13 Time evolution of a single row of the CCD for run 21 101
5.14 Time evolution of a single row of the CCD for run 22 at $T = 300$ K . 102
5.15 Time series for run 24. 104
5.16 Time series for run 113 at CHESS 105
5.17 $S(\vec{q}, t)$ vs t for run 21 107
5.18 $S(\vec{q}, t)$ vs t for run 22 108
5.19 $S(\vec{q}, t)$ for three different times after the quench. 111
5.20 Slices of $S(\vec{q}, t)$ for $qx = 0$ in model A 112
5.21 Time dependence of the fit parameters for model A 113
5.22 Time series of $S(\vec{q}, t)$ for $\vec{q} = (qx, 0)$ 115
5.23 $S(\vec{q}, t)$ vs t for several wavevectors. 116

TABLES

2.1 Experimental parameters 20
2.2 Brightness and coherence lengths for different sources 21

3.1 Characteristics of detectors 49

5.1 Experimental parameters for different quenches. 96

List of common symbols

R_s	distance source-sample.
R_{slit}	distance source-source x-y slits.
R_d	distance sample-detector.
R_c	distance sample-collimating pinhole.
D	collimating pinhole diameter.
l_z	longitudinal coherence length.
l_x	horizontal transverse coherence length.
l_y	vertical transverse coherence length.
l_s	typical speckle size.
d_{sx}, d_{sy}	horizontal and vertical source size.
d_{slit}	source x-y slits opening.
d_p	pixel size, 22.4μm.
$\Delta q_p = \frac{2\pi d_p}{\lambda R_d}$	$\vec{q}$ space increment.
τ	exposure time.
$V(\vec{r}, t)$	digital signal measured at position $\vec{r} = \vec{r}_{ij}$ between time t_k and $t_k + \tau$. $\vec{r}_{ij}$ and t_k are discrete due to the nature of the detection process.
$n_i(\vec{r}, t)$	incident number of photons on the surface of a pixel $\vec{r}$ at t as measured by a reference detector having near unit detective quantum efficiency.
$n_d(\vec{r}, t)$	detected number of photons.
$\alpha = \frac{<n_d>_t}{<n_i>_t}$	detective quantum efficiency of the detector.
$<V(\vec{r}, t)>_t = \frac{1}{N} \sum_{i=1}^{N} V(\vec{r}, t_i)$	time average of signal V. It is measured by averaging a time sequence of N scans.
$S^2_{t,V}(\vec{r}) = \frac{1}{N-1} \sum_{i=1}^{N} (V(\vec{r}, t_i) - <V(\vec{r}, t)>_t)^2$	estimator for the variance of V, measured with a time sequence of N scans.
$<V(\vec{r}, t)>_{\vec{r}} = \frac{1}{N_p} \sum_{i=1}^{N_p} V(\vec{r}_i, t)$	spatial average of signal V. It is measured by averaging N_p pixels in a given scan at time t.
$S^2_{\vec{r},V}(t) = \frac{1}{N_p-1} \sum_{i=1}^{N_p} (V(\vec{r}_i, t) - <V(\vec{r}, t)>_{\vec{r}})^2$	estimator for the variance of N_p pixels.
$2\theta_{\parallel}$	detector angle with respect to the incident beam direction, measured in the scattering plane.
$2\theta_{\perp}$	detector angle measured perpendicular to the scattering plane.

Résumé

Cette thèse est la première mesure de spectroscopie des fluctuations d'intensité (SFI) de la dynamique d'une transition de type ordre-désordre dans un alliage binaire, utilisant des rayons X cohérents. Des faisceaux intenses de rayons X cohérents de quelques μm de diamètre sont maintenant produits en filtrant spatialement et en fréquence des rayons X émis par une source synchrotron de troisième génération. Des patrons de diffraction tacheté de la surstructure (100) du Cu_3Au ont été mesurés avec un détecteur bi-dimensionel de type CCD. Pour mesurer les fluctuations temporelles et spatiales du facteur de structure, la résolution spatiale et la réponse du détecteur furent mesurées.

Nous avons développé une technique d'application générale, basée sur une comparaison de la moyenne, variance et corrélation spatiale du signal avec des fluctuations d'intensité suivant une loi de Poisson. Les corrélations spatiales du signal réduisent les fluctuations du signal détecté par rapport au bruit de Poisson prévu. Cette technique permet de mesurer la fonction de résolution et l'efficacité quantique du détecteur. La largeur de la fonction d'autocorrélation spatiale des patrons de diffraction tachetés est en accord quantitatif avec la largeur d'un patron de diffraction de Fraunhofer des trous, élargi par la fonction de résolution du CCD. Le contraste du patron tacheté est plus faible que prévu. La grandeur caractéristique des taches et leur contraste dépendent des propriétés optiques du faisceau et de la taille du trou utilisé comme prévu.

Nous avons mesuré des patrons tachetés après une trempe de l'état désordonné fcc à l'état ordonné $L1_2$. Les taches dominantes apparaissent rapidement après la trempe, mais reste fixe dans l'espace réciproque. La croissance des domaines est mesurée par un accroissement de l'intensité moyenne et un rétrécissement de la largeur du pic. Cette dynamique est en accord avec des simulations numériques du modèle A. L'amplitude des fluctuations est faible et leur durée est très longue. Nous avons démontré que la SFI est réalisable dans une nouvelle bande d'énergie. La SFI est un nouvel outil pour l'étude des phénomènes hors d'équilibre dans les solides.

Abstract

We extended Intensity Fluctuation Spectroscopy (IFS) to atomic scale fluctuations using coherent X-rays. Intense beams of coherent X-rays, with diameters of a few μm, are now easily produced by *spatial filtering* of *monochromatic* X-rays generated from synchrotron radiation insertion devices. This thesis is the first X-ray IFS measurement on the non-equilibrium dynamics of an order-disorder phase transition in a binary alloy. Speckle patterns of Cu_3Au (100) were measured with a two-dimensional Charge-Coupled Device detector. To quantify the spatial and temporal fluctuations of the speckle pattern, the spatial resolution and the noise of this detector were carefully characterized.

We developed a statistical technique for characterizing position-sensitive detectors (PSD), using estimators such as the average, variance, and *spatial correlation functions*. Spatial correlations between pixels reduce the fluctuations of the signal when compared to Poisson noise. Using this technique, the resolution function and quantum efficiency of two PSD's were measured. The widths of spatial correlation functions of static speckle patterns from Cu_3Au agree well with the widths of the Fraunhofer diffraction of the pinholes used, convolved with the detector resolution. The speckle pattern contrast is smaller than expected. The speckle size and contrast depend on the incident X-ray optics as expected for X-ray speckle.

We measure Cu_3Au speckle patterns after a quench from the fcc disordered phase to the $L1_2$ ordered phase. The dominant speckles appear after the quench, and remain *fixed* in reciprocal space. The domain coarsening is seen as an overall increase in intensity and a sharpening of the diffuse peak. These dynamics agree with numerical simulations of model A. Both experiments and simulations show that the time fluctuations of the intensity have small amplitudes and very long time scales. This differs from equilibrium IFS, where fluctuations amplitudes are as large as the signal. We have demonstrated the feasibility of XIFS in Cu_3Au. The use of coherent X-rays allows one to measure the ordering kinetics of binary alloys in new ranges of length and time scales.

Acknowledgments

I wish to thank Prof. Mark Sutton for introducing me to a very exciting field of research. I had the privilege of participating in the first coherent X-ray experiments with a world leader in the field. I would like to thank Mark for his constant intellectual stimulation and technical support throughout my stay at McGill. He always anticipated my computational needs, and provided me with the tools that made the work possible. This thesis benefitted from his careful reading and constructive criticism. I would like to thank him especially for taking me on very nice trips around the world, in countries where the wine and cheeses were wonderful!

I wish to thank also Dr. Brian Stephenson whose vast synchrotron experience was invaluable for this project. I have always enjoyed participating in experiments with him, and his visits to Montreal were important for the data analysis. I am grateful to Dr Brian Rodricks for providing the CCD detector and the detector expertise. Just a few years ago, very few people had or even used CCD detectors for X-ray scattering. We were very fortunate to have him in the team. A superb team of scientists helped to perform these experiments: Dr. Lonnie Berman, Dr. Randy Headrick, Dr. Carol Thompson, Prof. Simon Mochrie, Dr. Glen Held and Dr. S.E. Nagler. Thank you all!

I wish to acknowledge the close collaboration of Dr Ralf Brüning on the detector calibration section. With Ralf's help, my writing skills have improved, and his constructive criticisms were always appreciated. I am eternally grateful to my dear friend Geoff Soga for the careful editing of the thesis, often done at very short notice! I wish to acknowledge the collaboration of Dr. Ken Elder and Dr. Bertrand Morin on the data analysis of numerical simulations of model A.

A special thank is addressed especially to my teachers at McGill. Teaching is an essential but thankless task. I benefitted from the courses I took from Profs. Martin Grant, Peter Grütter, Martin Zuckermann, John Ström-Olsen, and Hong Guo.

My work benefitted from the excellent computer administrators who did an outstanding job over the years with often limited resources. Thanks to Loki Jorgensen, Martin Lacasse, Geoff Soga, Paul Mercure and Juan Gallego. Thank you for all the computer tips you gave me, and for fixing the system so professionally. My data analysis benefitted from many excellent computer programs written by M. Lacasse and M. Sutton.

Special thanks goes to the technical staff of the department. John Egyed, Michel Champagne, Frank van Gils, Saviero Biunno, Mario della Neve and Michel Beauchamp helped me in many experiments. Many thanks also to Paula Domingues, Diane Koziol, Joanne Longo, Cynthia Thomas and Lynda Corkum for making dealings with the department both simple and always pleasant.

I have enjoyed the intellectual stimulation and the friendship of many people at McGill. Thanks to the old timers in my group, Jacques, Yushan, Tianqu, Steve, Ralf, Hank, and to my present colleagues, Randa , Biao Hao, and Matt for many very stimulating discussions where I always learned something. I also enjoyed discussions and good times with my office mates and friends of room 422: Bian, Ming Mao, Erol, Claude, Mohsen, Christine, Morten, Ningjia, Stéphane, James, Sajan, Ke Xin, Bertrand... During my stay at McGill, I had the pleasure to meet wonderful people who made my stay in Montreal, an experience to remember: Geoff, Brett, Joel, Ling, Nick, Martin L., Martin K., Pascal, Eugenia, Judith, Mikko, Nicolas, Mary D., Karim, Ross, Ian, Jian Hua, Benoit, Philip, Niri , Francois, Margerita, Mark S., Martin Z., Martin G., Peter, Louis... I will miss you all!

I would like to thank Mark Sutton for supporting me financially. I am also very grateful for the scholarships I received from the Natural Sciences and Engineering Council of Canada et le Fonds pour la Formation des Chercheurs et l'Aide à la Recherche du Québec. In these time of budgetary restraint, I feel sad that young people today who are starting their graduate degrees might not have the same opportunities as I had several years ago.

J'aimerais remercier mes parents pour m'avoir laissé choisir librement ma voie dans la vie. Merci aussi pour votre aide financière et votre support moral pendant toutes ces longues années à étudier. Finally, I wish to express my gratitude to Mary Mardon for totally supporting my decision to go into graduate studies and research. Watching her battling the demons of her own dissertation alone and without the many resources that are available to people in the sciences has both inspired me and made me more aware of the intellectual and moral support that I have been lucky enough to receive. I would especially like to thank her for putting her own dissertation on hold this summer and fall, so that I could complete mine. I hope to offer the same support to you that you offered to me. I could not have done it without you.

Intensity fluctuation spectroscopy with coherent X-rays

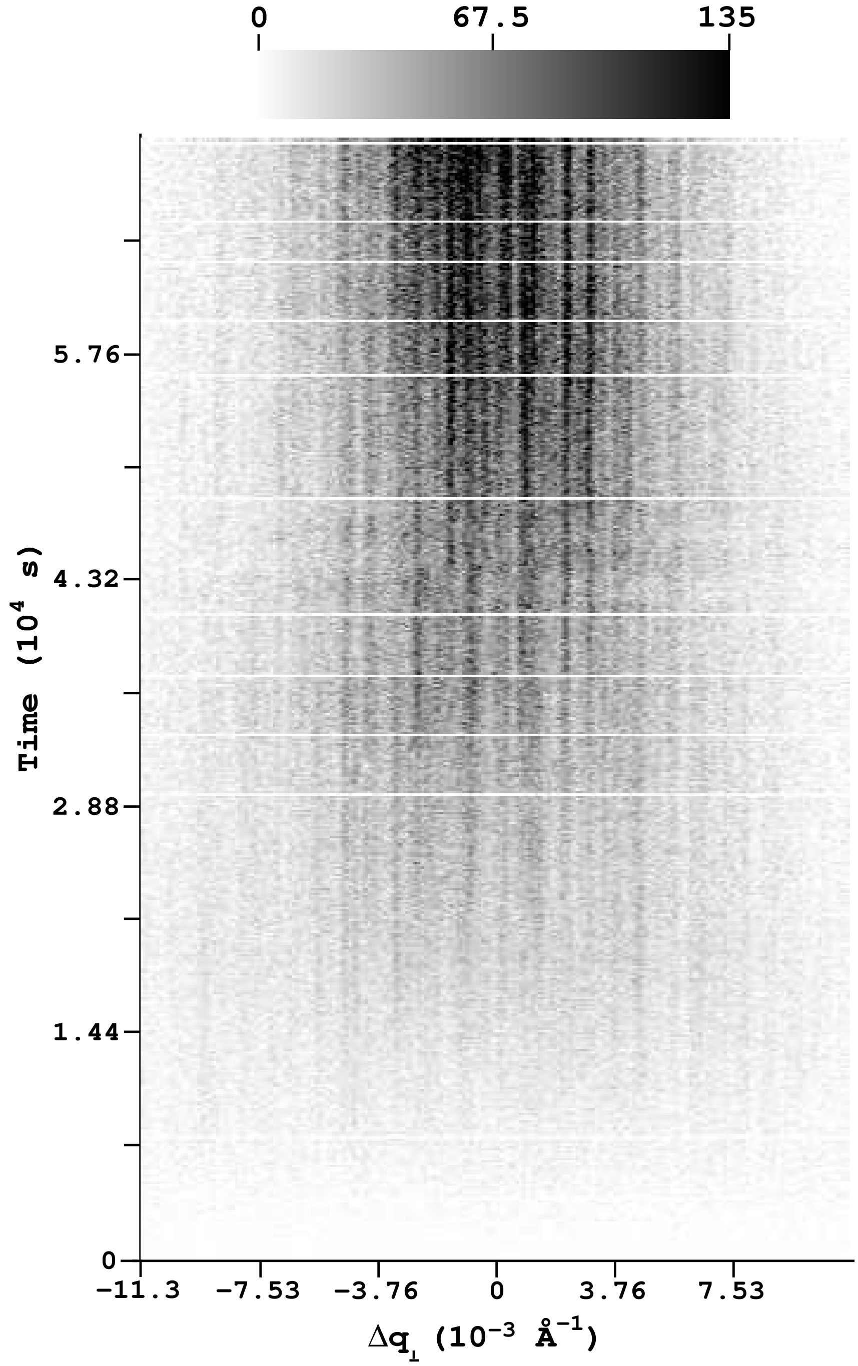

1

INTRODUCTION

The development in the last 30 years of high energy synchrotron rings dedicated to the production of synchrotron radiation has made possible many exciting new fields of science and technology. This high energy physics *technology* is used today by molecular biologists, chemists, physicists, medical doctors and engineers to find solutions to both fundamental and applied problems. In the field of solid-state physics, these sources have made many X-ray spectroscopy or scattering techniques feasible or more powerful. Some examples include time-resolved X-ray scattering, nuclear X-ray scattering, surface X-ray scattering, resonant and non-resonant X-ray scattering, Diffraction Anomalous Fine Structure (DAFS), coherent X-ray scattering, as well as many more[1]. This thesis will report on one of these recent developments which uses the high brilliance and transverse coherence of synchrotron radiation in X-ray scattering experiments. This transverse coherence greatly affects the observed X-ray diffraction patterns from disordered materials.

When coherent light illuminates a material with a random microstructure, a graininess in the scattered beam is observed, called speckle. Speckle is a general feature of scattered coherent light from a medium where some dielectric constant fluctuations are present. It was first observed over a century ago by Exner[3, 4] and Laue[5] on Fraunhofer diffraction rings produced by light scattered from small particles. It is seen in many experimental systems: in laser light reflected by a rough surface[2], in the

[1] See the wide variety of scientific projects investigated in modern synchrotron radiation facilities like the European Synchrotron Radiation Facility or the National Synchrotron Light Source in their respective Annual Reports [1, 2].

[2] In this case, speckle is considered as a nuisance that must be minimized to reveal the surface profile [6].

scattered light from equilibrium density fluctuations in a fluid, and in electron microscope images from amorphous semiconductors[1]. It is a characteristic of the *theoretical* structure factor of a random system where the fluctuations are caused by phasons in a quasi-crystal [8, 9, 10], phonons [11] and charge density waves in a perfect crystal, and in simple models of metallic glasses [10].

A speckle pattern is caused by coherent interference between all the scattered secondary waves randomly phase shifted by different regions of the material. If these regions move in time with characteristic time τ_c, then the intensity correlation function of the scattered light for a given scattering wave-vector $\vec{q}$, $< I(\vec{q},t)I(\vec{q},t+\delta t) >_t$, will decay with a characteristic time related to τ_c. Understanding the functional dependence of the correlation time on the momentum transfer allows for the study of transport properties of a material.

For example, the equilibrium intensity fluctuations of dilute spherical particles in a simple liquid follow $< I(\vec{q},t)I(\vec{q},t+\delta t) >_t \propto 1 + e^{-2Dq^2\tau}$, where D is the diffusion constant of the spheres in the liquid and q is the wavevector [12]. A plot of $1/\tau_c$ versus q^2 allows a measurement of the transport properties of the material. Using the Stokes approximation, $D = k_B T/(6\pi\eta a)$, where k_B is the Boltzmann constant, T the temperature, η the viscosity of the liquid, and a the sphere's average radius [12]. Thus by using spherical particles with a known radius a, one can measure the temperature dependence of the viscosity by measuring the temperature dependence of D, or by measuring the radius of some particle in a solution of known viscosity.

This time correlation technique, often called Dynamic Light Scattering (DLS), Intensity Fluctuation Spectroscopy (IFS), or Photon Correlation Spectroscopy (PCS)[2] has been used extensively with visible light to study the dynamics of very slow equilibrium and non-equilibrium fluctuations in *transparent* fluids, colloids and liquid crystals undergoing continuous phase transitions. This technique studies fluctuations with frequencies ranging from 10^{-3} to 10^8 Hz and length scales ranging between 2000 Å and 20 μm [14, 13]. It is complementary to inelastic light scattering tech-

[1] See Ref. [7] and references within.

[2] For an introduction to IFS, see the book by B. Chu[13], and references within.

niques like Brillouin and Raman scattering, which study faster processes ($10^7 - 10^{14}$ Hz) involving respectively acoustic and optical waves in materials. This technique has been limited to length scales above 200 nm when using lasers with the shortest wavelength available. The largest wavevector observable with visible light scattering is $q_{max} = (4\pi/200)$ nm^{-1}, which corresponds to back scattered light. This technique has been recently extended to hard X-rays by using high brilliance second generation synchrotron radiation sources, thus improving the technique sensitivity to *atomic* length scales with $q_{max} \approx (4\pi/0.1)$ nm^{-1}.

Sutton et al.[15] demonstrated that by appropriately collimating an incoherent monochromatic source of X-rays like an X-ray insertion device[1], one can get sufficient coherent flux to perform IFS at atomic length scales, through *opaque* materials. This first demonstration showed time independent speckle patterns from antiphase domains in Cu_3Au (100) [15]. Since this first demonstration, static speckle patterns have been observed in different systems: in gold coated diblock copolymer films[16], in synthetic multilayers[17], in the superlattice peak of a charge density wave in the one-dimensional conductor $K_{0.3}MoO_4$ [18], and in another binary alloy Fe_3Al[19, 20].

Sutton et al. also demonstrated the feasibility of X-ray IFS (XIFS) in a study of the kinetics of an order-disorder phase transition in Cu_3Au after a quench from the high temperature disordered phase to the low temperature ordered phase by measuring the fluctuations of the scattered intensity with a scintillation counter [21]. Within the last year, XIFS experiments have been performed successfully on the equilibrium critical fluctuations of the binary alloy Fe_3Al[19] and in equilibrium fluctuations in gold colloids[22, 23]. Brauer et al. [19] performed XIFS at atomic length scales, observing intensity fluctuations when the Fe_3Al sample was heated above the critical temperature of the continuous phase transition. Dierker et al. [22] have measured exponential correlation functions, characteristic of the Brownian motion of gold particles in a colloid with excellent signal to noise ratio. Chu et al. [23] also observed XIFS on a gold colloid using X-ray produced by a bending magnet beamline, with

[1] An insertion device is a periodic magnetic structure used to generate synchrotron radiation.

a coherent flux several orders of magnitude smaller than Ref. [22]. These recent experiments show the power and promise of this new field of X-ray scattering. This new technique promises to be quite helpful in studying the equilibrium and non-equilibrium dynamics in binary alloys, in amorphous materials and molten metals, in liquid crystals, in complex fluids like colloids and polymer blends, in gel networks, and in incommensurate systems like charge density wave or ferroelectric systems.

IFS is well understood for equilibrium fluctuations, but little experimental work has been performed using IFS on the non-equilibrium coarsening dynamics of a first order phase transition. One of the only other studies of coarsening in a first-order transition with dynamic light scattering was done on a binary fluid (conserved order parameter), where the intensity fluctuations were studied after quenches into the miscibility gap. Kim et al. [24] found that the power spectrum of the scattered intensity $P(f)$ measured after the quench was non-Lorentzian, following $P(f) \propto \exp(-|f|/f_0)$, with $f_0 < 0.1$ Hz. This power spectrum appeared to be stationary because it was present in the power spectrum of different consecutive subsets of their data. Hydrodynamic effects complicated the analysis of the intensity fluctuations in this system by increasing the droplet growth exponent by a factor of five, and causing oscillation in $P(f)$.

A simpler system for studying the intensity fluctuations due to the coarsening dynamics of a first order phase transition would be a system with a non-conserved order parameter (NCOP) like a binary alloy. Such a system would be free of hydrodynamic effects, and should be easier to understand because of the absence of conservation laws.

This thesis reports on the first study of the ordering kinetics of an order-disorder phase transition in a binary alloy with *coherent X-rays.* We measure the scattered intensity fluctuations from the superlattice peak (100) of Cu_3Au, after a quench from the equilibrium disordered state above the critical temperature T_c of the first order phase transition, to the degenerate ordered state below T_c. The speckle patterns of Cu_3Au generated by coherent illumination of the sample are measured with a charge-coupled device (CCD) array. The main advantage of the CCD array is to record hundreds of two dimensional speckle patterns, with a spatial resolution which matches the fine speckle features, and with a time resolution of tens of seconds to a few minutes [25], which is sufficient to measure the speckle pattern dynamics.

The binary alloy Cu_3Au was chosen because it is a classical system for the study of a first-order phase transition. It has been studied for over half a century[1]. The equilibrium properties of this system are analogous to a three dimensional Ising model with antiferromagnetic coupling. Furthermore, the non-equilibrium ordering kinetics of Cu_3Au has been studied extensively with incoherent illumination in recent years [28, 29, 30, 31, 32, 33]. After a quench through the order-disorder transition, nucleation and growth of ordered domains occur[2]. After nucleation, the late stage dynamics is controlled by curvature driven growth with the average domain size $R_d \propto t^{1/2}$. The scaling properties of the incoherent structure factor are well established and are universal features of ordering. The spherically averaged structure factor scales as $S(q,t) = t^{d/2} f(qt^{1/2})$, where d is the dimensionality, and $f(x)$ is a universal scaling function.

The theoretical foundation of IFS with non-equilibrium phenomena is not as well understood as its equilibrium counterpart. Therefore, it is important both experimentally and theoretically to develop an understanding of these phenomena. Another motivation for this thesis is to investigate the non-self averaging behavior of first-order phase transitions[36]. Roland and Grant [36] predicted $1/f$ noise in the fluctuations around scaling for a macroscopic quantity like the average domain size, in analogy with self-organized criticality. This is believed to be a universal feature of first-order phase transitions.

In Chapter 2, we review some of the important concepts of coherence and scattering with coherent X-rays. Most of this terminology was developed in the last thirty years by light scatterers, but may be unfamiliar to scientists specialized in the fields of X-ray or neutron scattering. In Chapter 3, we develop statistical techniques for

[1] The order-disorder transition in Cu_3Au is discussed in several X-ray scattering books [26, 27]

[2] Excellent reviews are given in Ref. [34, 35].

characterizing position-sensitive detectors (PSD) which were inspired from our data analysis of speckle patterns in Cu_3Au. In this work, it was essential to separate the noise due to counting statistics from genuine intensity fluctuations, and to develop an understanding of the inherent spatial correlations of the detected signal in a PSD in order to estimate the speckle size. This work has been published recently [37]. Chapter 4 discusses the experimental method used for this work, expanding points developed earlier in Chapter 2. In Chapter 5, results from static and time-dependent measurements are reported, and compared to numerical simulations.